

Electronic Supplementary Materials (ESI) for:

Substituent Effects on the Redox States of Locally Functionalized Single-Walled Carbon Nanotubes revealed by *in situ* Photoluminescence Spectroelectrochemistry

Tomonari Shiraishi,¹ Tomohiro Shiraki,^{1,2*} Naotoshi Nakashima^{2*}

¹ Department of Applied Chemistry, Graduate School of Engineering, Kyushu University, 744 Motoooka, Nishi-ku, Fukuoka 819-0395, Japan

² International Institute for Carbon-Neutral Energy Research (WPI-I2CNER), Kyushu University, Fukuoka, Japan.

Email: shiraki.tomohiro.992@m.kyushu-u.ac.jp; nakashima.naotoshi.614@m.kyushu-u.ac.jp

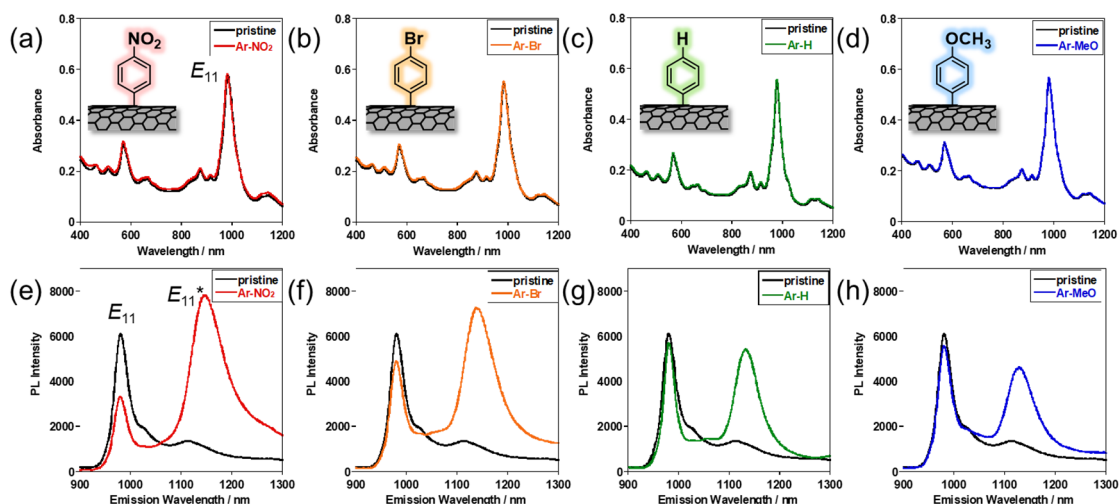


Fig. S1 (a, b, c and d) Absorption and (e, f, g and h) PL spectra of the (black) pristine and (-NO₂: red, -Br: orange, -H: green and -MeO: blue) Ar-X-SWNTs, in which the SWNTs were solubilized in D₂O containing 0.20 wt% SDBS.

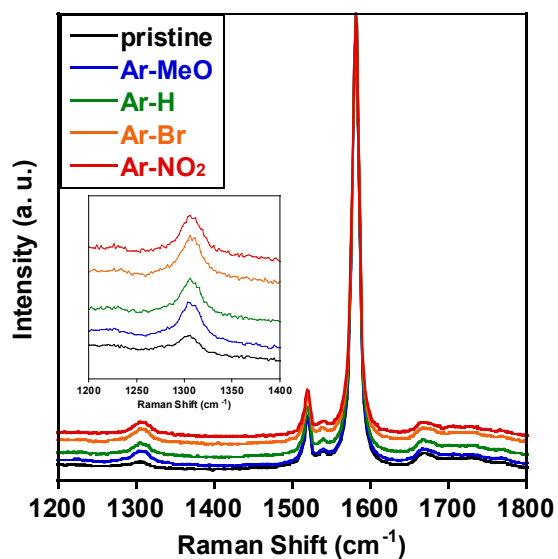


Fig. S2 Raman spectra of (black) pristine, (blue) Ar-MeO, (green) Ar-H, (orange) Ar-Br and (red) Ar-NO₂-SWNTs dissolved in 0.20 wt% SDBS aqueous solutions. Excitation wavelength is 532 nm.

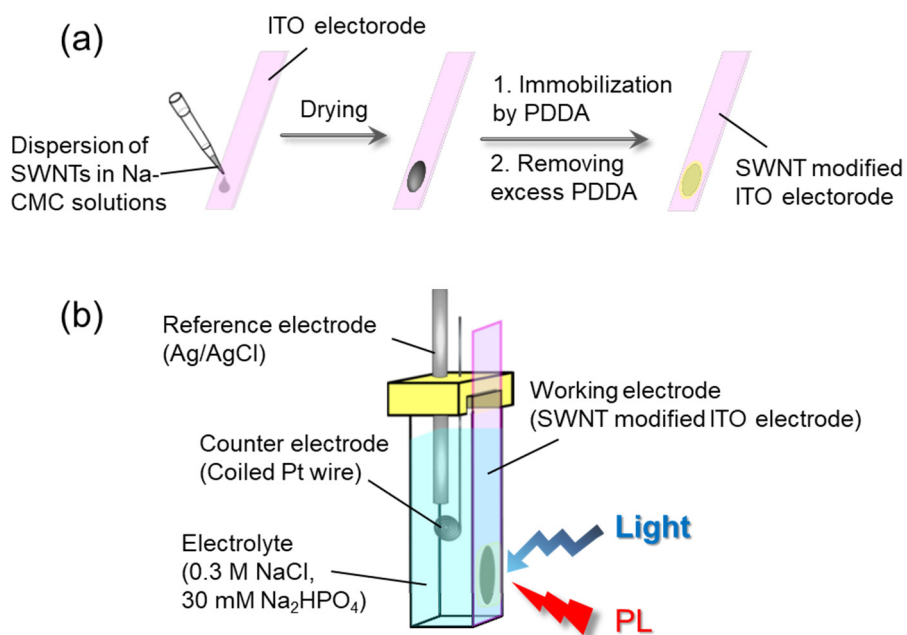


Fig. S3 Schematic depiction for (a) the preparation of an SWNT-modified ITO electrode and (b) *in-situ* PL electrochemical measurement setup.

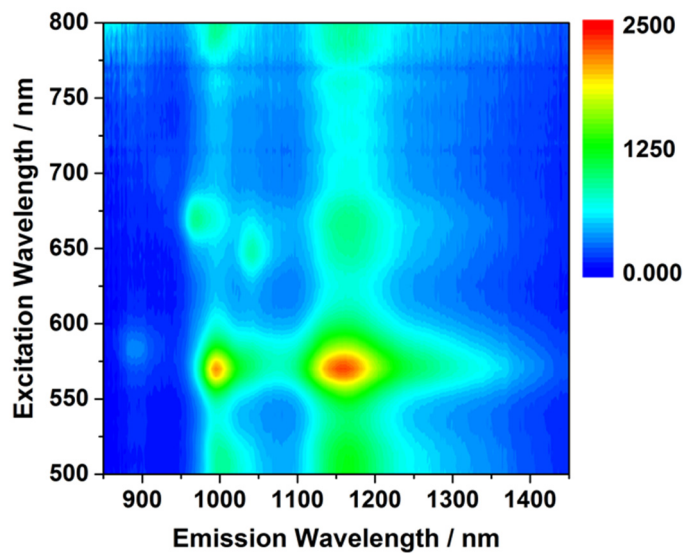


Fig. S4 2D-PL mapping of the film containing isolated Ar-NO₂ SWNTs on an ITO electrode.

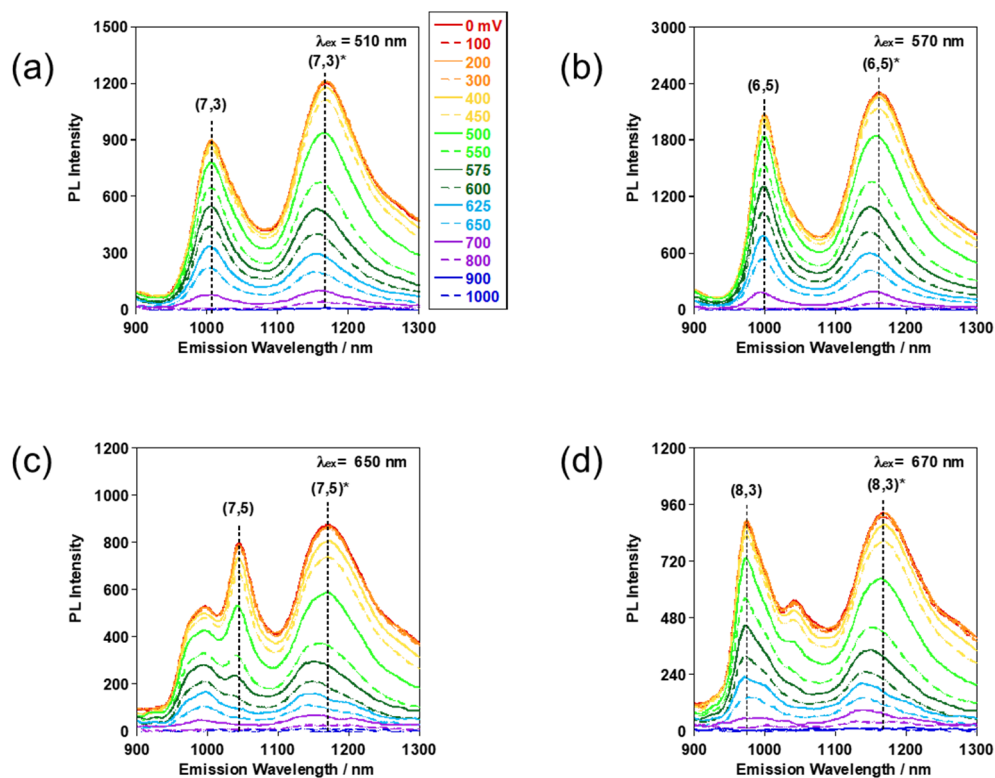


Fig. S5 Applied potential (from 0 to 1000 mV vs. Ag/AgCl)-dependent PL spectra of the Ar-NO₂-SWNTs. The PL spectra were measured by excitation at (a) 510, (b) 570, (c) 650 and (d) 670 nm.

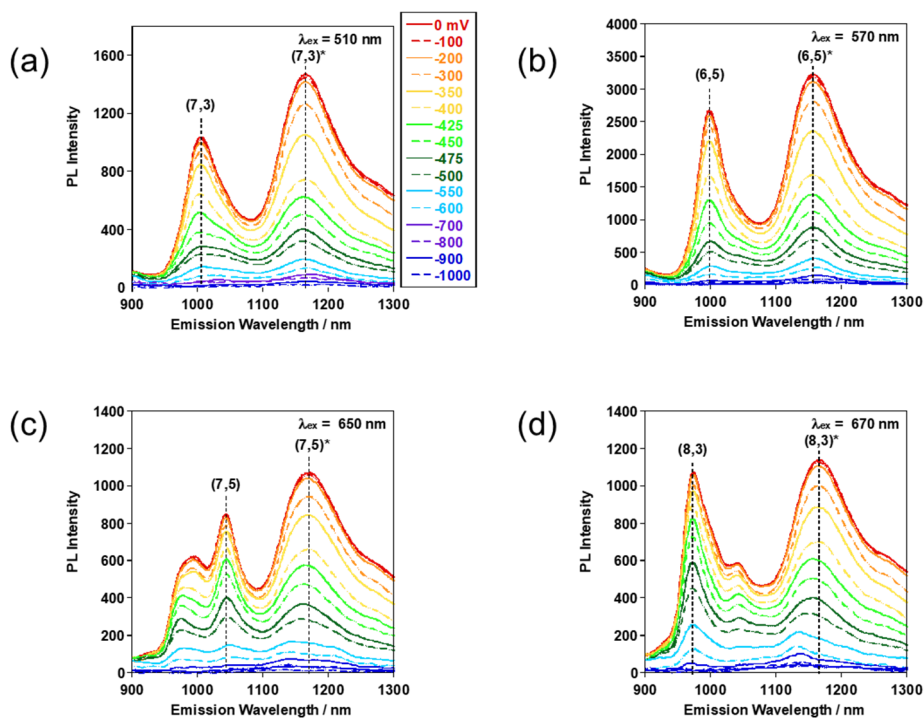


Fig. S6 Applied potential (from 0 to -1000 mV vs. Ag/AgCl)-dependent PL spectra of the Ar-NO₂-SWNTs. The PL spectra were measured by excitation at (a) 510, (b) 570, (c) 650 and (d) 670 nm.

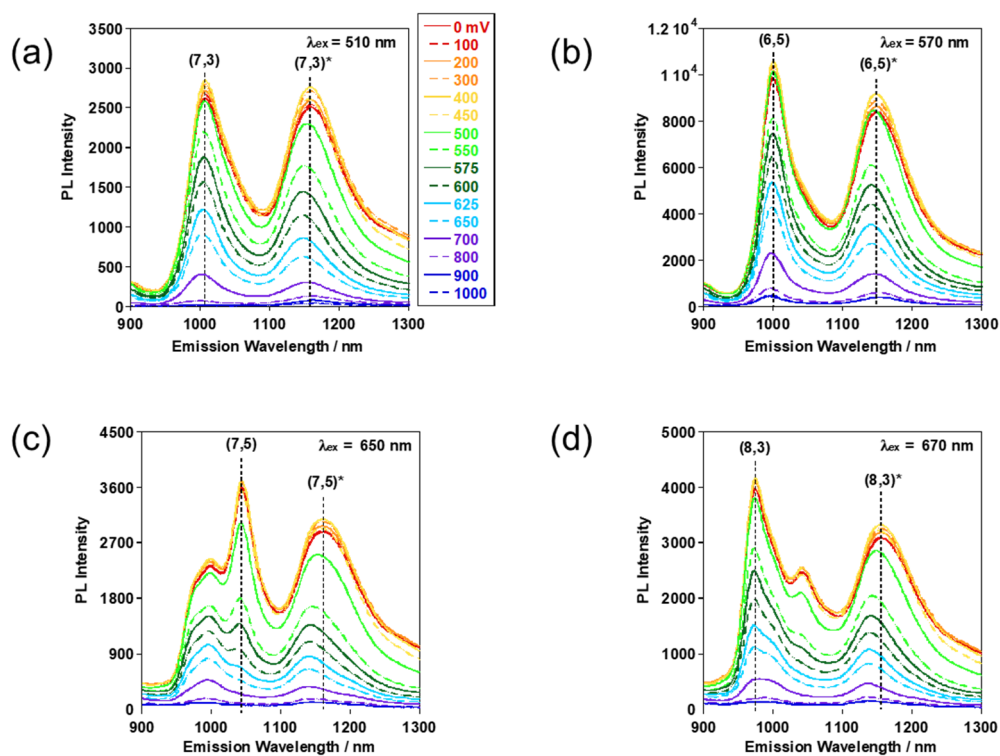


Fig. S7 Applied potential (from 0 to 1000 mV vs. Ag/AgCl)-dependent PL spectra of the Ar-Br-SWNTs. The PL spectra were measured by excitation at (a) 510, (b) 570, (c) 650 and (d) 670 nm.

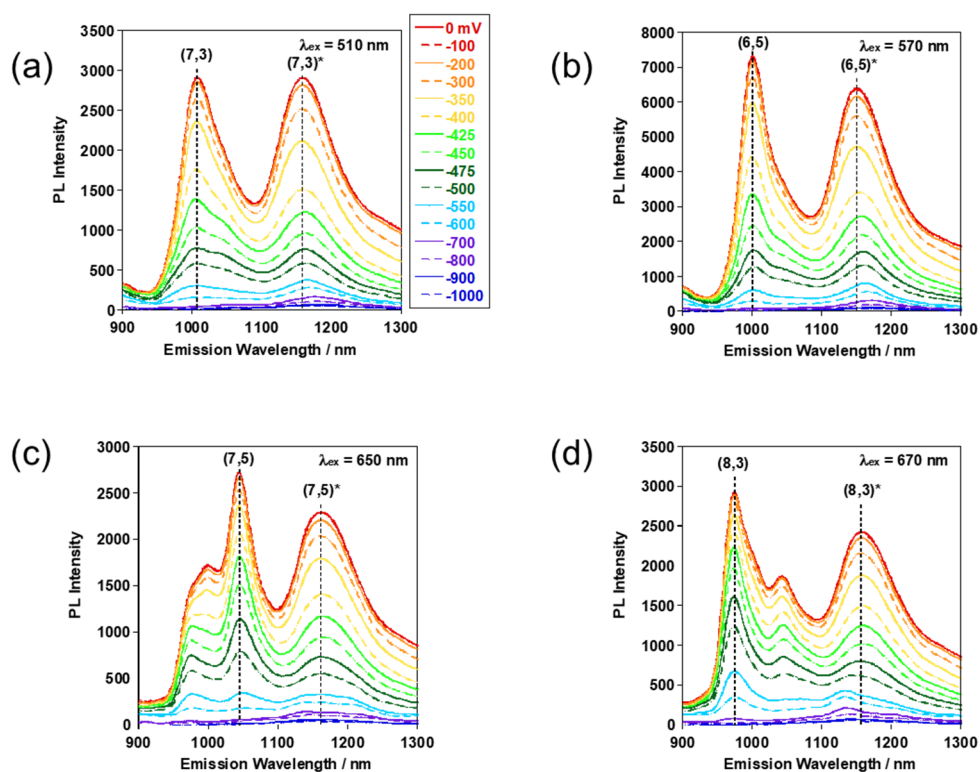


Fig. S8 Applied potential (from 0 to -1000 mV vs. Ag/AgCl)-dependent PL spectra of the Ar-Br-SWNTs. The PL spectra were measured by excitation at (a) 510, (b) 570, (c) 650 and (d) 670 nm.

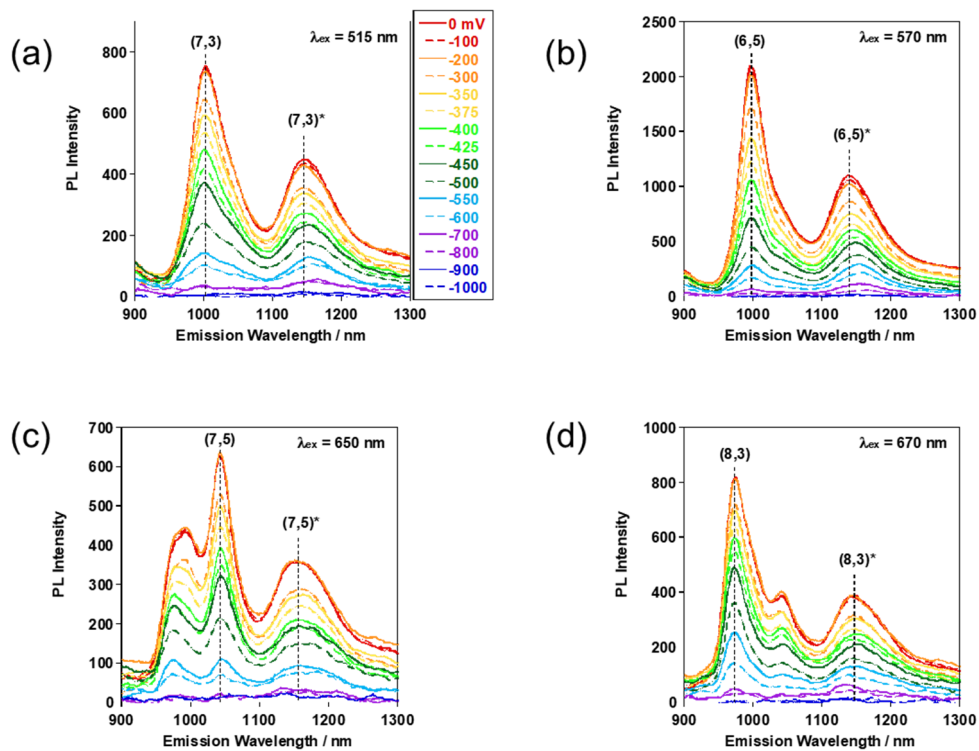


Fig. S9 Applied potential (from 0 to 1000 mV vs. Ag/AgCl)-dependent PL spectra of the Ar-H-SWNTs. The PL spectra were measured by excitation at (a) 515, (b) 570, (c) 650 and (d) 670 nm.

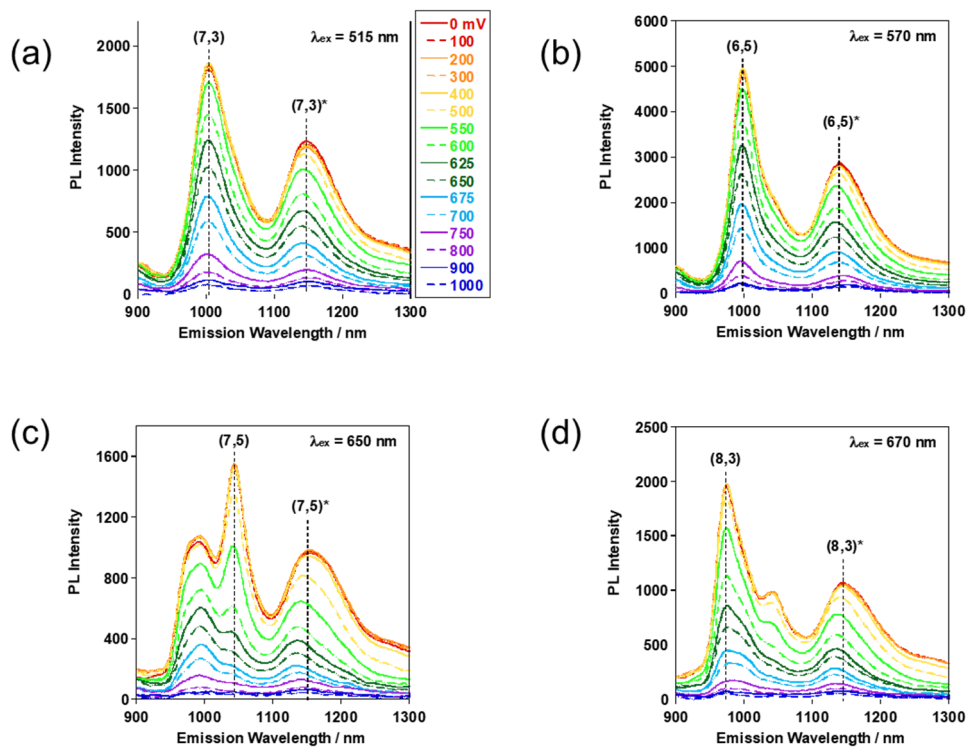


Fig. S10 Applied potential (from 0 to -1000 mV vs. Ag/AgCl)-dependent PL spectra of the Ar-H-SWNTs. The PL spectra excited at (a) 515, (b) 570, (c) 650 and (d) 670 nm.

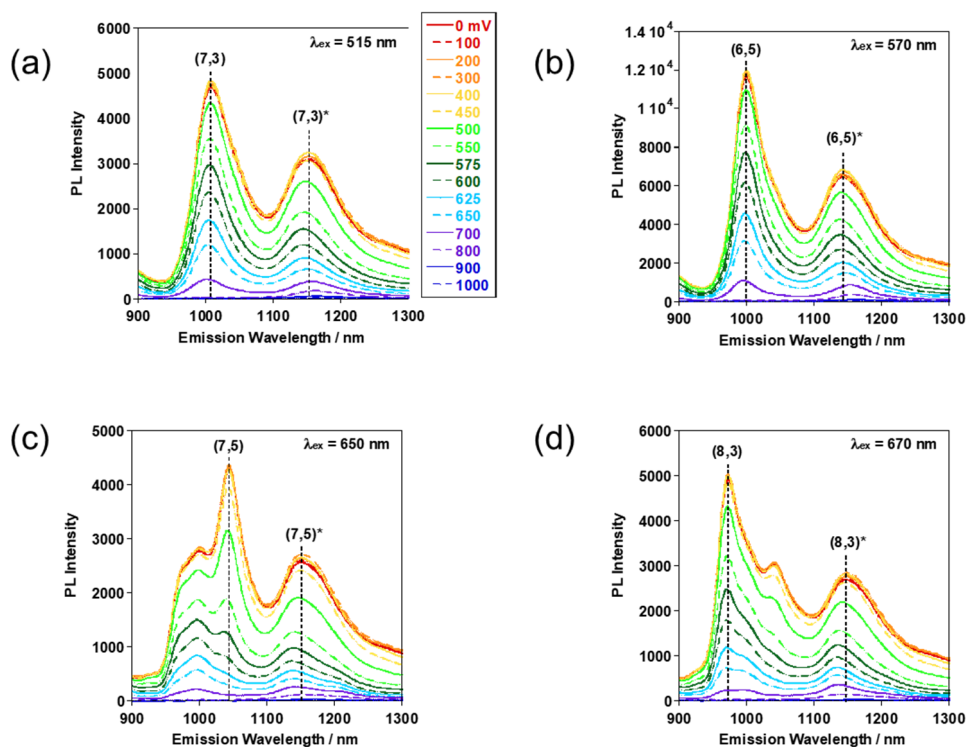


Fig. S11 Applied potential (from 0 to 1000 mV vs. Ag/AgCl)-dependent PL spectra of the Ar-MeO-SWNTs. The PL spectra were measured by excitation at (a) 515, (b) 570, (c) 650 and (d) 670 nm.

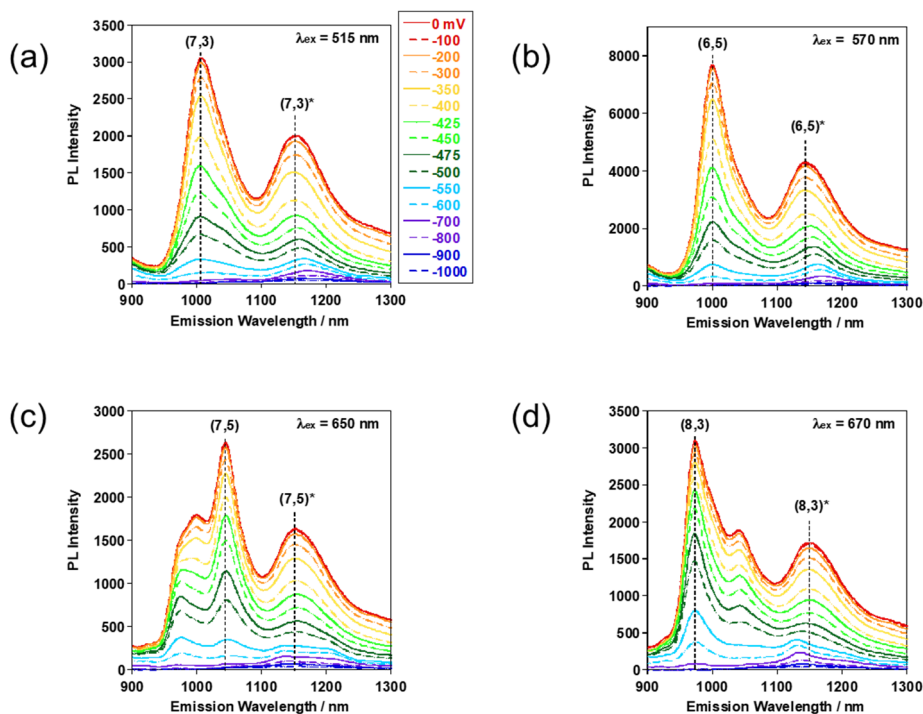


Fig. S12 Applied potential (from 0 to -1000 mV vs. Ag/AgCl)-dependent PL spectra of the Ar-MeO-SWNTs. The PL spectra were measured by excitation at (a) 515, (b) 570, (c) 650 and (d) 670 nm.

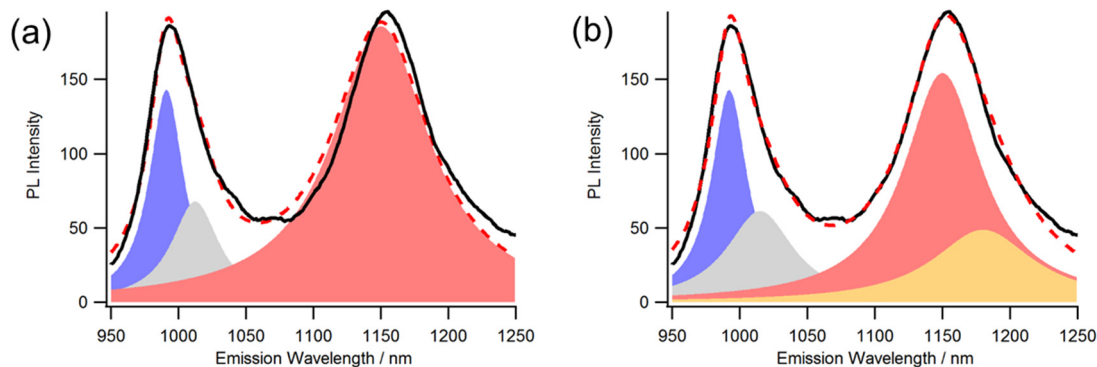


Fig. S13 Deconvoluted PL spectra of the Ar-NO₂-SWNTs film on an ITO electrode at 700 mV. The deconvolution was conducted (a) without and (b) with consideration of the trion PL. The black lines and dashed red lines are the original measured spectra and the fitting curves obtained from combining the deconvoluted spectra, respectively. The colored areas show the E_{11} peak (blue area), the E_{11}^* peak (red area), PL from the SWNTs with the other chiralities (gray area) and the trion PL (orange area). $\lambda_{\text{ex}} = 570$ nm. The trion peak for (6,5)SWNTs was reported to appear at 1170 nm when oxidation and reduction potentials exceeded 600 mV and -500 mV, respectively.^{S1} In the PL results measured over those applied potentials, elimination of the trion emission provided proper fitting results in the deconvolution process. For the other SWNTs with $(n,m) = (7,3)$, $(7,5)$, and $(8,3)$ chiralities, trion elimination was conducted in the same manner. In this measurement condition, other new peaks assignable to localized trion that may be generated at the defect sites are not recognized.

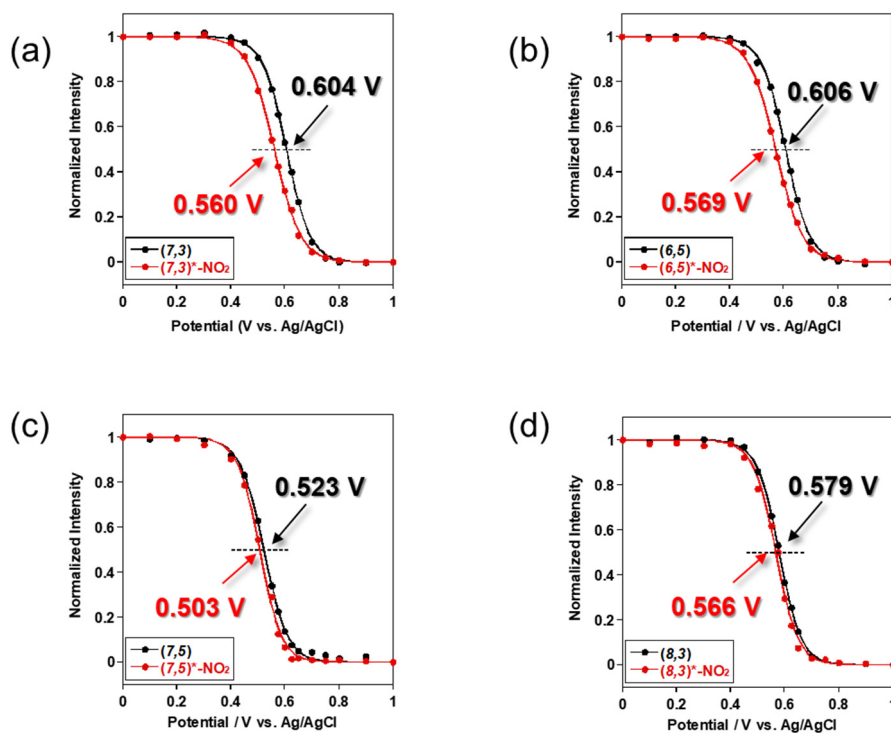


Fig. S14 Normalized PL intensity plots as a function of applied potentials in the oxidation process. The colored lines represent E_{11} (black) of the non-doped SWNTs and E_{11}^* (red) of the Ar-NO₂-SWNTs.

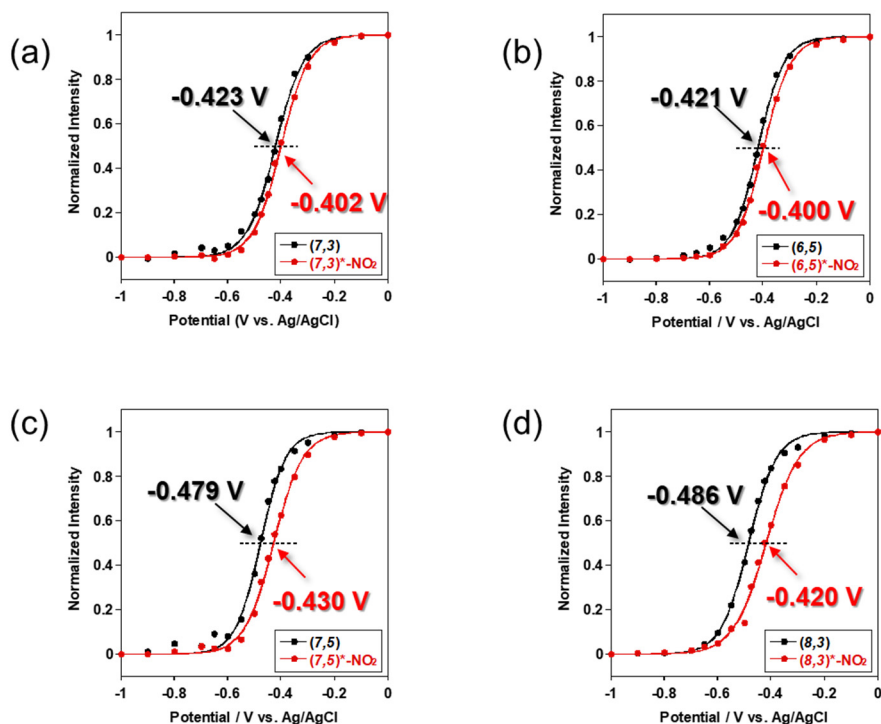


Fig. S15 Normalized PL intensity plots as a function of applied potentials in the reduction process. The colored lines represent E_{11} (black) of the non-doped SWNTs and E_{11}^* (red) of the Ar-NO₂-SWNTs.

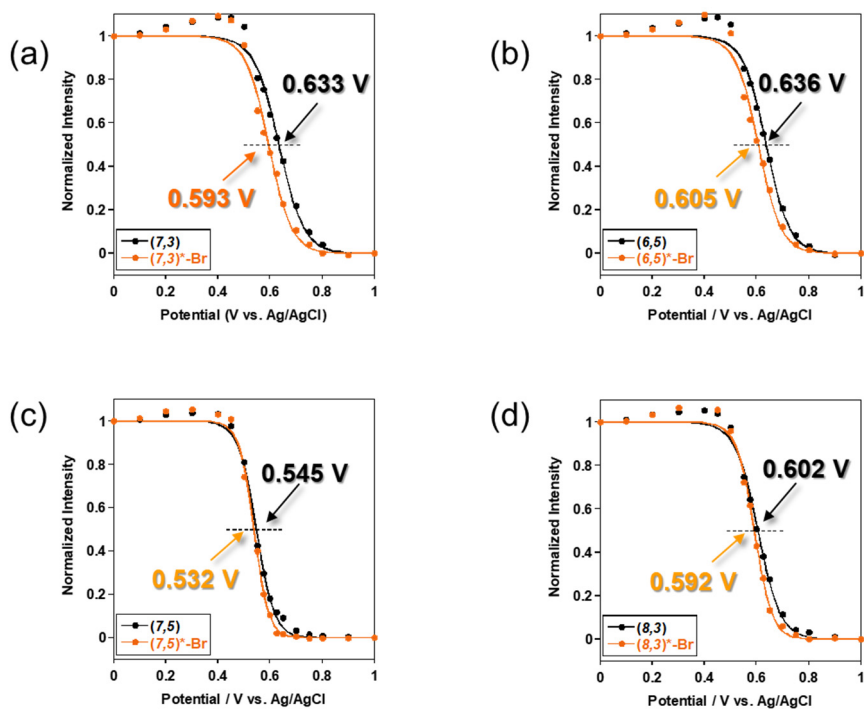


Fig. S16 Normalized PL intensity plots as a function of applied potentials in the oxidation process. The colored lines represent E_{11} (black) of the non-doped SWNTs and E_{11}^* (orange) of the Ar-Br-SWNTs.

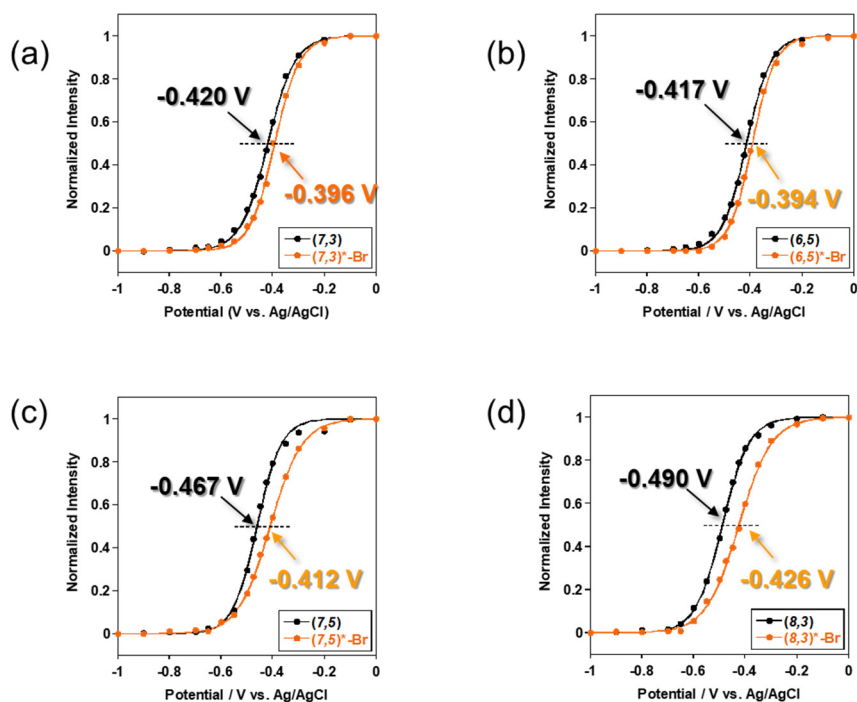


Fig. S17 Normalized PL intensity plots as a function of applied potentials in the reduction process. The colored lines represent E_{11} (black) of the non-doped SWNTs and E_{11}^* (orange) of the Ar-Br-SWNTs.

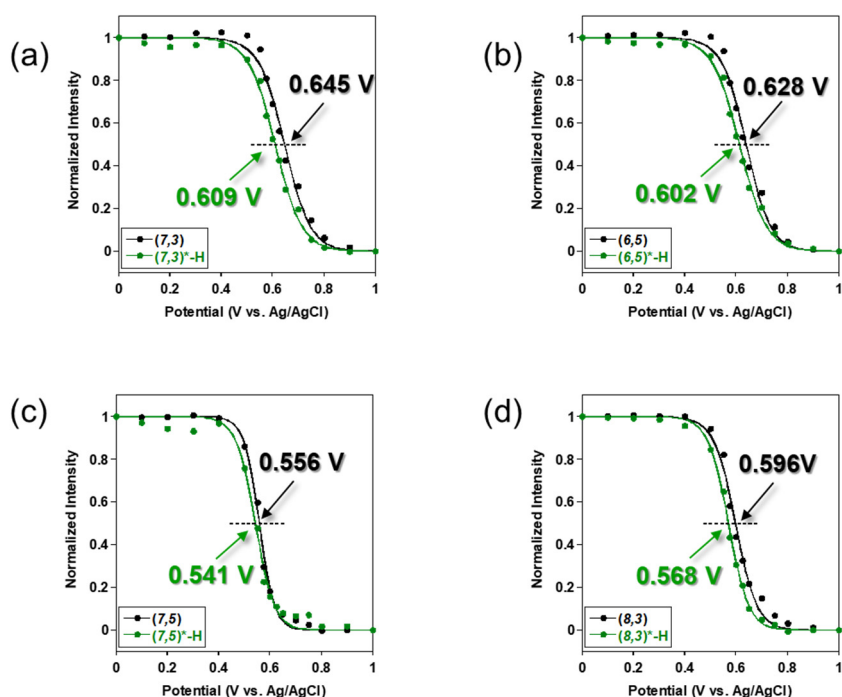


Fig. S18 Normalized PL intensity plots as a function of applied potentials in the oxidation process. The colored lines represent E_{11} (black) of the non-doped SWNTs and E_{11}^* (green) of the Ar-H-SWNTs.

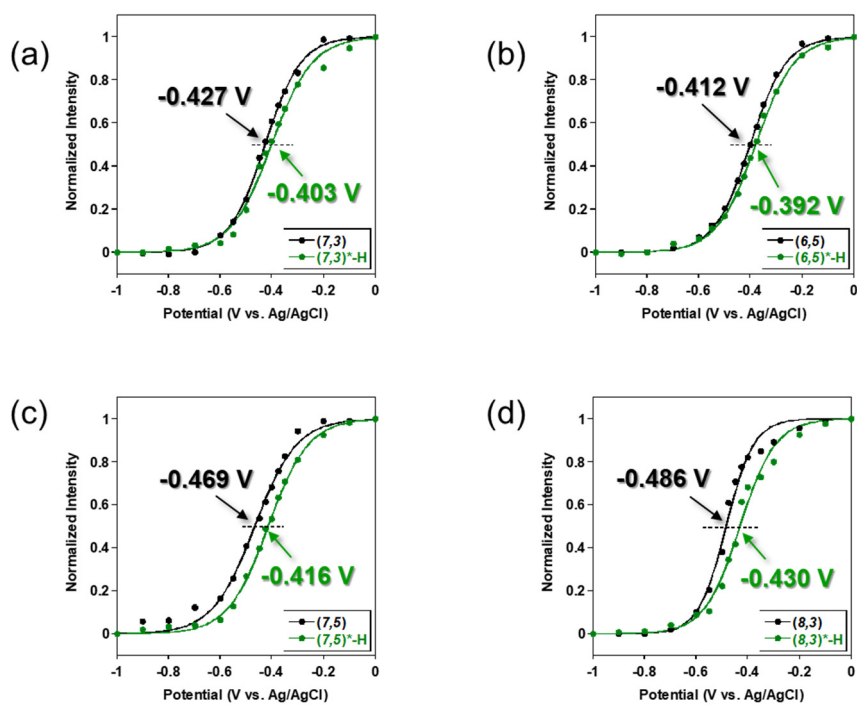


Fig. S19 Normalized PL intensity plots as a function of applied potentials in the reduction process. The colored lines represent E_{11} (black) of the non-doped SWNTs and E_{11}^* (green) of the Ar-H-SWNTs.

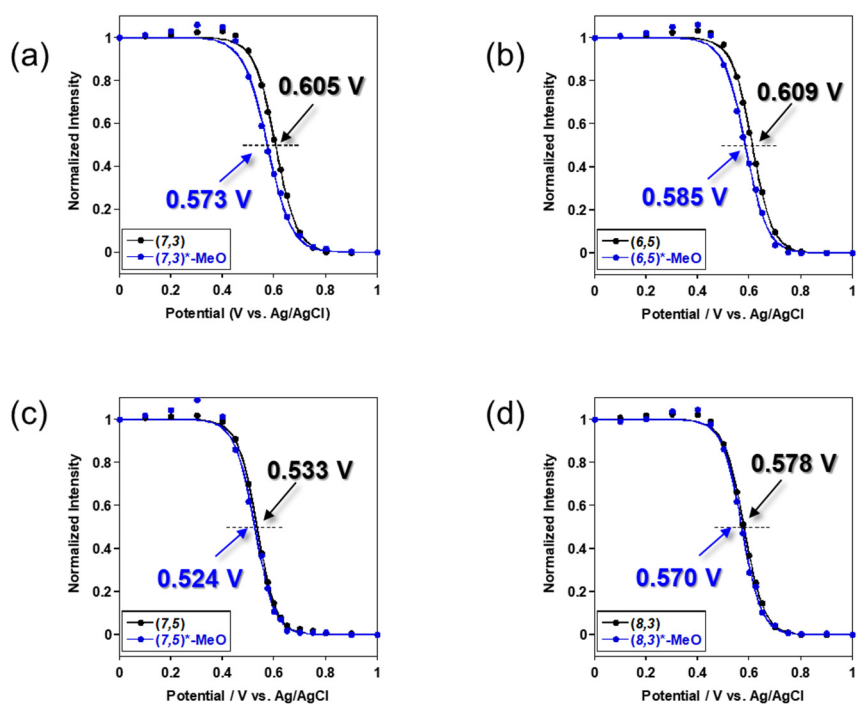


Fig. S20 Normalized PL intensity plots as a function of applied potentials in the oxidation process. The colored lines represent E_{11} (black) of the non-doped SWNTs and E_{11}^* (blue) of the Ar-MeO-SWNTs.

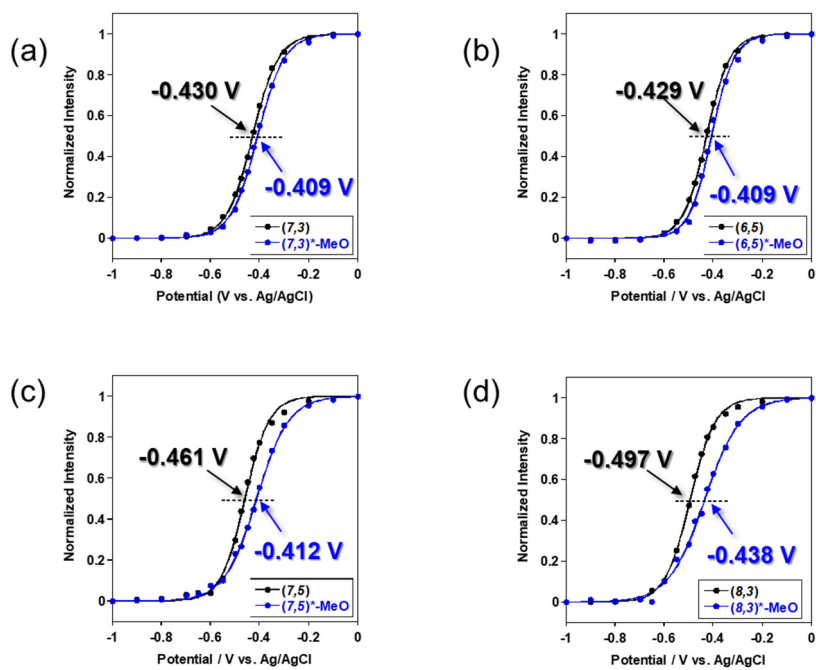


Fig. S21 Normalized PL intensity plots as a function of applied potentials in the reduction process. The colored lines represent E_{11} (black) of the non-doped SWNTs and E_{11}^* (blue) of the Ar-MeO-SWNTs.

Table S1 D/G area ratios of Ar-X-SWNTs. The values were determined from the Raman spectra shown in Figure S2.

	D/G area ratio
Pristine-SWNTs	0.0416
Ar-MeO-SWNTs	0.0854
Ar-H-SWNTs	0.0855
Ar-Br-SWNTs	0.1080
Ar-NO₂-SWNTs	0.1054

Table S2 Determined electronic properties of Ar-X-(*n,m*)SWNTs. These values are average of multiple measurements for each sample.

Chirality (<i>n,m</i>)	Ar-X SWNT	E_{ox} (V vs. Ag/AgCl)	E_{red} (V vs. Ag/AgCl)	Fermi level (V vs. Ag/AgCl)	ΔE_{opt} (meV)	$\Delta E_{electro}$ (meV)
(6,5)	Pristine	0.615	-0.420	0.098	1242	1035
	NO₂	0.578	-0.400	0.098	1072	978
	Br	0.584	-0.398	0.093	1082	982
	H	0.589	-0.400	0.095	1089	989
	MeO	0.593	-0.399	0.097	1091	992
(7,3)	Pristine	0.613	-0.424	0.095	1235	1037
	NO₂	0.569	-0.403	0.083	1068	972
	Br	0.573	-0.400	0.087	1076	973
	H	0.577	-0.400	0.089	1078	977
	MeO	0.581	-0.403	0.089	1086	984
(7,5)	Pristine	0.533	-0.468	0.033	1257	1001
	NO₂	0.515	-0.412	0.052	1126	927
	Br	0.516	-0.416	0.050	1132	932
	H	0.518	-0.417	0.051	1134	935
	MeO	0.526	-0.420	0.053	1141	946
(8,3)	Pristine	0.583	-0.490	0.047	1269	1073
	NO₂	0.538	-0.427	0.056	1053	965
	Br	0.547	-0.425	0.061	1063	972
	H	0.555	-0.434	0.061	1070	989
	MeO	0.557	-0.432	0.063	1076	989

Table. S3 Electronic properties of the pristine SWNTs reported in ref. 27.

Chirality (<i>n,m</i>)	E_{ox} (V vs. Ag/AgCl)	E_{red} (V vs. Ag/AgCl)	Fermi level (V vs. Ag/AgCl)	$\Delta E_{\text{electro}}$ (meV)
(6,5)	0.588	-0.423	0.083	1011
(7,3)	0.582	-0.420	0.081	1002
(7,5)	0.524	-0.454	0.033	978
(8,3)	0.556	-0.490	0.035	1046

Reference in ESI

S1 J. S. Park, Y. Hirana, S. Mouri, Y. Miyauchi, N. Nakashima and K. Matsuda, *J. Am. Chem. Soc.*, 2012, **134**, 14461-14466.